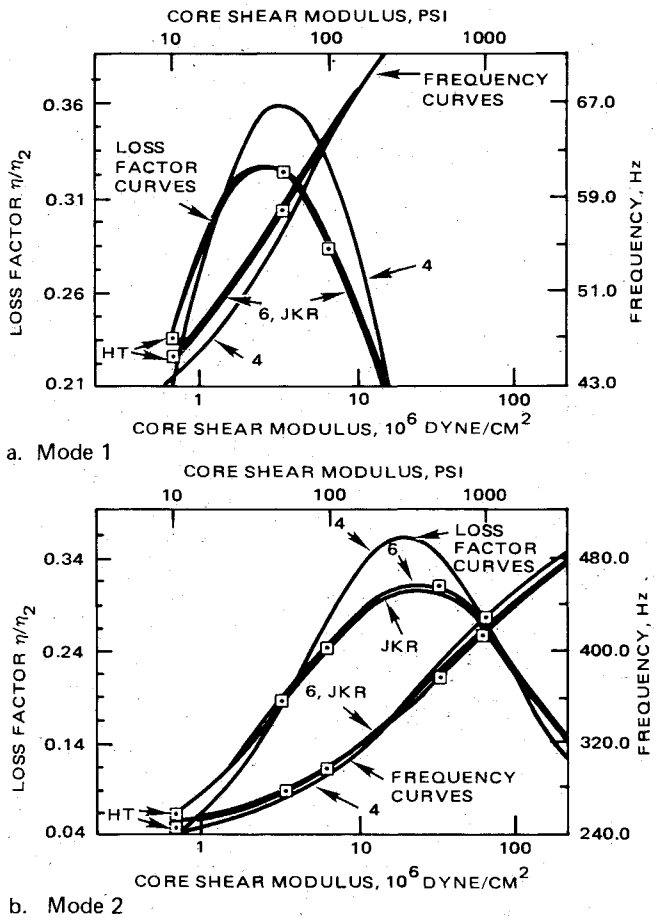

Fig. 4 Loss factors and natural frequencies for cantilever beam using the fourth- and sixth-order theories and the Johnson-Kienholz-Rodgers and Holman-Tanner finite elements.

the capability both to input a general stiffness matrix and to use the modal strain energy method. MSC/NASTRAN[5] has been used in this investigation. The model is generated in the conventional manner. More nodes provide the additional degrees-of-freedom required by these elements. These nodes coincide with the conventional element nodes, and their unused degrees-of-freedom are restrained. The required MSC/NASTRAN bulk data cards for these elements are created using a preprocessor. The input for this preprocessor is 1) connectivity cards identical to the CBAR and CQUAD4 cards, 2) property cards similar to the PBAR and PQUAD cards, and 3) GRID cards for the conventional element nodes. The output of this preprocessor is 1) the GENEL cards for the face sheet and core stiffness matrices, 2) the CONM2 cards for the lumped mass matrices, 3) the GRID cards for the locations of the additional nodes, and 4) the SPC cards for the restraints on the additional nodes.

The modal strain energy method can be used to efficiently solve this problem.[3] First, a standard modal extraction is executed and, then, the elastic strain energy in each element for each mode is calculated. Unfortunately, MSC/NASTRAN computes the strain energy in all elements except the GENEL element; nevertheless, MSC/NASTRAN's direct matrix abstraction programming (DMAP) capability can be used to compute the GENEL strain energies. The modal loss factors are then computed using Eq. (1). Finally, the modal loss factors are input via a damping vs frequency table for subsequent forced response calculations.

Results

To evaluate the accuracy of the finite element representation, a series of calculations was performed using both the finite element model and the analytical theory. A 178-mm (7.00-in.) long by 12.7-mm (0.50-in.) wide cantilever beam with 1.27-mm (0.050-in.) thick aluminum face sheets and a 0.127-mm (0.005-in.) thick core was used in the analysis. The dimensions of this beam were those of the standard test specimen used to obtain material properties of viscoelastics by controlled vibration. The core's loss factor was held constant at 0.01 and its shear modulus was varied through a wide range of values.

The results are presented in Fig. 4 for the first two cantilever modes obtained from the fourth-order theory of Ross et al.,[1] the sixth-order theory of Rao,[2] and twenty element NASTRAN models, using the Johnson-Kienholz-Rodgers[3] and the Holman-Tanner[4] finite elements. The results are given for the modal loss factor η, normalized with respect to the core loss factor η_2, and the natural frequency. The sixth-order theory and the NASTRAN results are in excellent agreement, while those for the fourth-order theory differ somewhat, as was expected in view of the assumptions used in its derivation.

References

[1] Ross, D., Ungar, E. E., and Kerwin, E. M. Jr., "Damping of Flexural Vibrations by Means of Viscoelastic Laminae," *Structural Damping*, Sec. III, ASME, New York, 1959.

[2] Rao, D. K., "Frequency and Loss Factors of Sandwich Beams Under Various Boundary Conditions," *Journal of Mechanical Engineering Science*, Vol. 20, May 1978, pp. 271-282.

[3] Johnson, C. D., Kienholz, D. A., and Rodgers, L. C., "Finite Element Prediction of Damping in Structures with Constrained Viscoelastic Layers," *Proceedings of the 51st Symposium on Shock and Vibration*, San Diego, Calif., Oct. 1980.

[4] Holman, R. E. and Tanner, J. M., "Finite Element Modeling Techniques for Constrained Layer Damping," AIAA Paper 81-0485, April 1981.

[5] McCormick, C. W., *MSC/NASTRAN User's Manual Version 60*, The MacNeal-Schwendler Corp., Los Angeles, Calif., 1980.

Buckling of Very Thin, Nearly Perfect Axially Loaded Circular Cylindrical Shells

C. G. Foster*
University of Tasmania, Hobart, Tasmania, Australia

Introduction

THE complex problem of predicting buckling loads for axially compressed cylindrical shells has defied any completely adequate explanation. Traditionally, the discrepancy between the classical load and the vast amount of experimental data available (e.g., as summarized by Hart-Smith[1]) has been attributed to end conditions and defects. The defects may be due to geometrical, metallurgical, or loading inconsistencies. However, very thin, expertly made shells (e.g., those of Babcock and Sechler[2]) collapse at loads substantially less than those predicted when end constraints are taken into account. A plausible explanation for this discrepancy is offered in terms of the space frame analogy for axial compression buckling previously developed by the author.[3-5]

Received Aug. 26, 1981; revision received June 24, 1982.

*Senior Lecturer in Mechanical Engineering.

Space Frame Analogy

The buckling mode for cylindrical shells loaded in axial compression consists of a series of dimples. Yoshimura[6] showed that this mode was an almost developable surface which could be approximated by a series of flat triangular facets. When a model of the Yoshimura buckle pattern is examined it is readily apparent that the structure is capable of withstanding a substantial load. Also, that load cannot be carried over the entire facet. For equilibrium it is necessary that a stress concentration exists near the fold lines of the Yoshimura pattern and in the direction of the fold line. Thus, the load carrying portion of the Yoshimura pattern can be represented by a space frame as illustrated in Fig. 1. In this model there are diagonally oriented compression members and (for equilibrium) tangential members which are in tension. The members are angle members with the flanges of the angles located in the planes of the facets. The members are essentially pin ended and have an effective width W which is dependent on the stress distribution in the facet.

The space frame analogy relies on examining the buckling behavior of a space frame representing the cylinder. The size of the facets in the equivalent Yoshimura pattern is taken as the size of the controlling defect in the buckling cylinder. The buckling load is calculated as the load to collapse one of the diagonal compression members of the frame.

Buckling Process

Tennyson[7] has demonstrated by high-speed photography of isoclinic fringes in high quality epoxy shells that axisymmetric rings can occur at the point of collapse. Embedded in the rings were small fringes which were apparently due to the formation of dimples. These dimples eventually interacted to become the well known Yoshimura pattern. The small dimples could in themselves be considered to behave in the same manner as shape defects. If the space frame analogy is applied with facets of the same size as the dimples then the large discrepancy between theory and experiment for cylinders with very high radius to thickness ratios disappears.

Perfect cylinders loaded completely axisymmetrically may not show the dimples mentioned in the preceding paragraph. However, in actual test situations, some inconsistency in loading inevitably exists. These inconsistencies can be expressed as a combination of various mode shapes and the amplitude of each of the modes will increase until the deflections due to the most significant mode become large enough for the structure to collapse. The situation is further compounded in that when nonlinearities are present, deformations in one mode may promote the formation of another mode which in turn causes the collapse. This condition appears to be the case in very thin cylinders. Initially, the axisymmetric mode forms and the deformations associated with this mode promote dimples which spread to form the Yoshimura pattern. The size of the dimples is such that the length of a facet is half the wavelength of the axisymmetric deformation. In very thin cylinders collapse of a Yoshimura buckle pattern of this size occurs at a load less than that required to collapse the cylinder axisymmetrically.

From previous work the aspect ratio of the facets in the Yoshimura pattern can be given by

$$\lambda = L2/L1 = 1.606 - 0.121 \ell n(R/T) \tag{1}$$

where $L1$ is the circumferential length of the triangular facets in the buckle pattern, $L2$ the axial developed length of the facet, R shell radius, and T the shell thickness.

Now, because the dimples occupy the space between the axisymmetric rings, their overall length ($2L2$) can be given by the critical length of the classical buckling mode.

$$2L2 = \frac{2\pi (RT)^{1/4}}{\{12(1-\nu^2)\}^{1/4}} \tag{2}$$

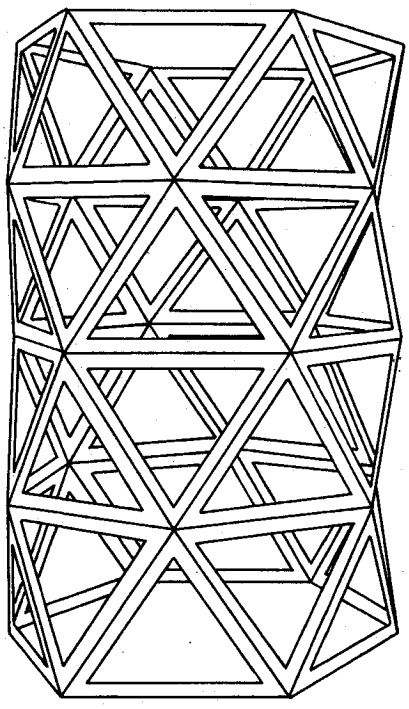

Fig. 1 Space frame representation.

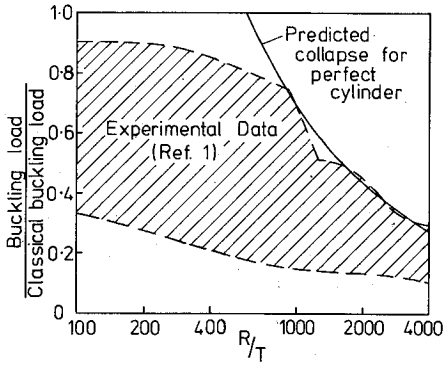

Fig. 2 Comparison of predictions with experimental evidence.

When Eq. (1) is substituted in Eq. (2) we find that the circumferential length of dimples is given by

$$L1 = 2\pi R/N = \frac{\pi (RT)^{1/2}}{\{12(1-\nu^2)\}^{1/4}\{1.606 - 0.121 \ell n(R/T)\}} \tag{3}$$

From Eq. (3) the number of circumferential dimples (N) can be established and the space frame analogy can be used to predict the buckling load of near perfect shells.

The buckling load of the diagonal member ($P1$, tension positive) previously has been shown to be given by the relation

$$1 + \frac{16L1^2EWT\sin^2(\phi/4)}{P1\{L2^2 + (1.5L1)^2\}^{1.5}}\left[\{L2^2 + (L1/2)^2\}/2 - \frac{\tan([\{L2^2 + (L1/2)^2\}\{-P1/(EI)\}]^{1/2}/2)}{\{-P1/(EI)\}^{1/2}}\right] = 0 \tag{4}$$

In Eq. (4), E is Young's modulus, I the moment of inertia of the buckling member [Eq. (5)], and ϕ the angle that the tangential member subtends at the axis of the cylinder [Eq. (6)].

$$I=\frac{TW}{6}\left[\sin^2(\phi/4)\{L2^2+(L1/2)^2\}(W^2-T^2)/L2^2+T^2\right] \tag{5}$$

$$\phi=2\pi/N \tag{6}$$

From the work to date an effective width of flange of 21 times the thickness appears realistic.

The solution of Eq. (4) is multivalued. The lowest root (other than zero) corresponds to the fundamental buckling mode of the diagonal member and provides an estimate of the buckling load in that member. The total load on the cylinder (P) is then obtained from equilibrium conditions [Eq. (7)].

$$P=2NPI\left\{\frac{L2^2-(L1/2)^2\tan^2(\phi/4)}{L2^2+(L1/2)^2}\right\} \tag{7}$$

The load calculated from Eq. (7) using values of N given by Eq. (3) is plotted in Fig. 2 as a function of radius to thickness ratio. Since the discussion in this Note is centered around high quality shells where naturally occurring defects are very small we would expect that the calculated buckling loads would not be less than experimentally determined loads. Therefore, the theoretical curve should approximate the upper limit of experimental data. Figure 2 illustrates good correlation between the calculated values and the known experimental evidence for R/T values greater than 1000. The experimental loads never exceed the calculated values by more than 8% and except for radius to thickness ratios in the vicinity of 4000 the agreement is within about 3%.

Discussion

The space frame analogy was developed on the assumption that the ratio of effective width of flange of frame members to shell thickness remained constant. This clearly could not be the case in very small facets where the flanges could be considered larger than the facets. Facets of the size given by Eq. (2) are about the size where the flanges almost completely cover the entire facet (i.e., the calculations are made at about the upper limit of applicability of the analogy). Additionally, the aspect ratio relation quoted [Eq. (1)] was obtained from measured data for post-buckled configurations with a considerably smaller number of facets.

Even allowing for errors associated with the aspect ratio and the effective width of flange it is apparent that for very thin near perfect cylinders a substantial reduction in the buckling load from the classical load is a certainty. The reduction appears to be not just due to initial imperfections but rather a deformation mode developed during loading.

References

[1] Hart-Smith, L. J., "Buckling of Thin Cylindrical Shells under Uniform Axial Compression," *International Journal of Mechanical Science,* Vol. 12, April 1970, pp. 299-313.

[2] Babcock, C. D. and Sechler, E. E., "The Effect of Initial Imperfections on the Buckling Stress of Cylindrical Shells," NASA TN D1510, Dec. 1962, pp. 135-142.

[3] Foster, C. G., "Some Observations on the Yoshimura Buckle Pattern for Thin-Walled Cylinders," *Transactions of the ASME Journal of Applied Mechanics,* Vol. 46, June 1979, pp. 377-380.

[4] Foster, C. G., "Estimation of the Collapse Loads of Thin-Walled Cylinders in Axial Compression," *Transactions of the ASME Journal of Applied Mechanics,* Vol. 46, June 1979, pp. 381-385.

[5] Foster, C. G., "On the Buckling of Thin-Walled Cylinders Loaded in Axial Compression," *Journal of Strain Analysis for Engineering Design,* Vol. 16, July 1981, pp. 205-210.

[6] Yoshimura, Y., "On the Mechanism of Buckling of a Circular Cylindrical Shell under Axial Compression," NACA TM 1390, 1955.

[7] Tennyson, R. C., "Buckling Modes of Circular Cylindrical Shells under Axial Compression," *AIAA Journal,* Vol. 7, Aug. 1969, pp. 1481-1487.

Orthogonal Polynomials as Variable-Order Finite Element Shape Functions

Dewey H. Hodges*
U.S. Army Research and Technology Laboratories (AVRADCOM), Ames Research Center, Moffett Field, California

Introduction

VARIABLE-order finite element methods have an advantage over conventional finite element methods in that additional degrees of freedom may be added to the model without the need to generate a new element geometry. These additional element degrees of freedom generally are not physical displacements or rotations of some point at the element boundary. Instead, they are typically generalized coordinates associated with a set of polynomial shape functions of a variable order higher than that of the conventional polynominal shape functions used in defining the displacement field of the element in terms of displacements and rotations at the boundary. In some cases the variable-order polynomials may be organized so that the corresponding generalized coordinates may be displacements, rotations, or derivatives of displacement of some set of points within the element.

Previous papers[1,2] indicate that, when elements are chosen to be free of discontinuities in properties, for a given number of degrees of freedom in the total structure, higher accuracy is obtained using fewer elements with polynomials of higher order. For the range of problems investigated in Ref. 1, there are also corresponding improvements in computational effort. Results from the author's unpublished work in both static and dynamic, linear and nonlinear, and conservative and nonconservative problems indicate that the same trends hold for a wide class of one-dimensional problems.

Although the shape functions in Ref. 1 lead to well-conditioned element matrices for beams, the shape functions presented therein lack certain computational advantages.

1) The element matrices that result from the shape functions are not sparse.

2) The element matrices are not hierarchical; that is, matrices that result from shape functions of a given order are not submatrices of the ones obtained from shape functions of a higher order. This is because all the shape functions change each time the order is increased.

3) Since the variable-order shape functions contain displacements and rotations at the boundary, the corresponding generalized coordinates cannot be eliminated from the global equations in a linear static problem. The purpose of this Note is to present variable-order polynomial shape functions that overcome these disadvantages.

In typical applications of finite element methods, the unknown functions are expanded in a series of polynomials in each element and certain relationships are enforced at the element boundaries. For one-dimensional structures, the relationships may be either between values of the functions themselves or between values of the functions and first derivatives of the functions. The shape functions for the former are typically referred to as C0 type shape functions while the latter are C1 type. In this Note variable-order shape functions of both types are presented.

Received May 17, 1982; revision received July 20, 1982. This paper is declared a work of the U.S. Government and therefore is in the public domain.

*Research Scientists, Rotorcraft Dynamics Division, Aeromechanics Laboratory. Associate Fellow AIAA.